

General Disclaimer

One or more of the Following Statements may affect this Document

- This document has been reproduced from the best copy furnished by the organizational source. It is being released in the interest of making available as much information as possible.
- This document may contain data, which exceeds the sheet parameters. It was furnished in this condition by the organizational source and is the best copy available.
- This document may contain tone-on-tone or color graphs, charts and/or pictures, which have been reproduced in black and white.
- This document is paginated as submitted by the original source.
- Portions of this document are not fully legible due to the historical nature of some of the material. However, it is the best reproduction available from the original submission.

MICROWAVE RADIATION MEASUREMENTS NEAR THE ELECTRON PLASMA FREQUENCY OF THE NASA LEWIS BUMPY TORUS PLASMA

by R. Mallavarpu* and J. R. Roth

National Aeronautics and Space Administration
Lewis Research Center
Cleveland, Ohio 44135

ABSTRACT

Microwave emission near the electron plasma frequency of the NASA Lewis Bumpy Torus plasma has been observed, and its relation to the average electron density and the dc toroidal magnetic field was examined. The emission was detected using a spectrum analyzer and a 50 Ω miniature coaxial probe. The radiation appeared as a broad amplitude peak that shifted in frequency as the plasma parameters were varied. The observed radiation scanned an average plasma density ranging from $2 \times 10^{10} \text{ cm}^{-3}$ to $8 \times 10^{11} \text{ cm}^{-3}$. A linear relation was observed between the density calculated from the emission frequency and the average plasma density measured with a microwave interferometer. With the aid of a relative density profile measurement of the plasma, it was determined that the emissions occurred from the outer periphery of the plasma.

INTRODUCTION

Measurements of microwave radiation near the plasma frequency ω_{pe} have been reported from several plasma heating experiments. Wharton (1959) has observed microwave emission near ω_{pe} on fast, high current linear turbulent heating experiments. Attempts were made in that experiment to relate the intensity of radiation to the electron temperature. Strilchuk and Skarsgard (1973) report observing intense bursts of microwave radiation in the range from ω_{pe} to ω_{ce} from a miniature toroidal argon plasma experiment subject to a large electric field parallel to the confining magnetic field. Their experiment does not reveal any simple dependence of the radiation frequency on the

* National Aeronautics and Space Administration - National Research Council Research Associate.

discharge parameters. The radiation itself is accounted for by the interaction between a few energetic electrons and the main plasma. Schriver (1973), in linear turbulent heating experiments where the plasma is excited by applying electric fields along the plasma column, found a strong correlation between the time dependence of the plasma resistivity and microwave radiation near ω_{pe} . An estimate of the electron temperature was obtained from the energy dissipation due to the anomalously high resistivity. Oomens et al. (1976) describe a radiation spectrum ranging from 300 MHz to 5 GHz in low-density discharges in the Alcator experiment. The radiation was found to be strongly peaked near the ion plasma frequency, ω_{pi} , and the onset of this radiation was found to correlate strongly with the production of energetic ions. Also the electron density n_e as calculated by assuming the peak frequency to be ω_{pi} radiation was found to be roughly equal to the measured average electron density. Adati et al. (1977) conducted experiments on a turbulently heated theta pinch plasma and observed intense radiation near the electron plasma frequency, ω_{pe} . The power of the microwave radiation was found to be related to the plasma resistance R and it was suggested that the electromagnetic radiation was caused by nonlinear coupling between electron plasma waves and ion acoustic waves, or as a result of the linear conversion of the electron plasma waves due to a density gradient.

From a brief review of the literature described above, it is apparent that most of the experiments were conducted on turbulently heated, pulse excited plasmas. The aim of those experiments was to relate the microwave radiation in the plasma to an anomalous plasma resistance and to obtain an estimate for the electron temperature from the energy dissipation due to the high plasma resistivity. The onset of the radiation was usually correlated to the production of energetic ions or to the interaction of an energetic electron beam with the main plasma. No simple dependence of the microwave radiation near ω_{pe} on the plasma parameters was observed.

In this paper we report the observation of microwave radiation near ω_{pe} from the NASA Lewis Bumpy Torus plasma. The radiation frequency and the

density calculated from it are shown to vary proportionally with the measured average electron density, over a wide range of plasma density.

EXPERIMENTAL SYSTEM

The microwave radiation experiments near ω_{pe} , described in this paper, were conducted on the NASA Lewis Bumpy Torus plasma, a machine that operates in the steady state under the influence of a dc toroidal magnetic field and strong dc electric fields along the minor radius of the plasma. The electric fields heat the ions preferentially by $(E \times B)/B^2$ drift, and to a large extent determine the plasma stability and confinement properties. An isometric cut-away drawing of the NASA Lewis Bumpy torus facility is shown in figure 1. The 12 superconducting coils, each capable of 3 T on its axis, have a 19 cm inside diameter, and are arranged in a toroidal array 1.5 m in major diameter. The plasma is generated by biasing the midplane electrode rings between the coils to high positive or negative potentials with respect to the coils (Roth and Gerdin, 1976, 1977). Best particle confinement times and highest average densities were achieved with negative polarities and with only one electrode in operation (Roth and Gerdin, 1977; Roth, 1978). The best results were obtained when the electrode consisted of a 0.62 cm diameter water-cooled stainless steel rod along the minor diameter of the plasma, or a "D" shaped electrode surrounding the minor circumference of the plasma.

The apparatus used to detect microwave radiation from the plasma is shown schematically in figure 2. The detection system consists of a 1.5 m long, 50 Ω miniature coaxial line, one end of which is suitably shaped in the form of a straight wire or a circular loop. These two probe configurations have the same amplitude sensitivity above 100 MHz but the circular loop antenna has the advantage of being sensitive to the polarization of the incoming electromagnetic signal. The antenna is concentrically located in a reentrant quartz tube that is inserted into the vacuum tank through an airlock. The other end of the coaxial line leads to a spectrum analyzer capable of scanning the range 10 MHz to 18 GHz. The

length of the cable circuitry is kept at a minimum to avoid cable resonances and stray rf pickup.

The amplitude of the rf emissions was seen to depend on the distance of the coaxial antenna from the plasma boundary; orientation of the antenna with respect to the toroidal axis of the plasma; and proximity of the probe to the plasma region under the grounded coil dewars, where the electric fields are strongest. Figure 3 shows a series of signal traces for varying distances of the probe from the plasma boundary. The amplitude of the peak is greatest for the closest approach of the probe to the plasma boundary. Based on several rf emission experiments that were conducted on this plasma (Roth and Gerdin, 1976; Mallavarpu and Roth, 1977; Mallavarpu, 1977) it was determined that port 2 was the best location for the rf probe. Figure 4 shows the location of the rf probe with respect to the electrode ring, coil dewars, and the toroidal axis of the plasma. Lines of constant magnetic field strength are superimposed on the figure. The rf probe is located as close as possible to the region between the plasma and the inner bores of the coils, where the radial electric field is strongest.

EXPERIMENTAL RESULTS

The microwave radiation frequency near ω_{pe} was monitored as a function of the plasma parameters over a wide operating range. This emission appears on the spectrum analyzer as a broad amplitude peak that shifts in frequency when the operating parameters, such as electrode voltage and current, background gas pressure etc. are varied. A characteristic photograph of this emission peak for one set of plasma parameters is shown in figure 5. Experimental data were recorded for negative and positive electrode polarities. In the negative polarity case, the rod and "D" shaped electrode geometries were used. With positive electrode polarity, the radial electric field points outward in the vicinity of the rf probe; with negative polarity, the radial electric field points inward (Roth and Gerdin, 1977; Roth, 1978).

Negative Polarity

Figure 6(a) shows the peak emission frequency f , in Hertz, versus the average density $\langle n_e \rangle$ measured with a microwave interferometer. Figure 6(b) shows the density n_e obtained by assuming f to be the electron plasma frequency plotted against the measured $\langle n_e \rangle$, for the rod and "D" shaped electrode geometries. For the experimental data shown in these figures, the toroidal dc magnetic field was held at 2.4 T, the neutral background deuterium gas pressure at 7.4×10^{-5} torr, and the dc electrode current I_A was varied from 0.03 to 2.7 A. The data recorded scans an average density range from $2 \times 10^{10} \text{ cm}^{-3}$ to $8 \times 10^{11} \text{ cm}^{-3}$. In figure 6(a) the data is clustered along the line $f = \langle n_e \rangle^{1/2}$, indicating that the radiation frequency bears a square root relationship to the average density. Figure 6(b) shows that the electron density in the emitting region obtained by assuming $f = f_{pe}$ lies along the line $n_e = 4/11 \langle n_e \rangle$. The density in the emitting region is therefore lower than the average density by a factor of 2.75.

To find out the dependence of the emitting region location on the toroidal dc magnetic field B_T , the average density of the plasma was held constant while the radiation frequency was monitored as a function of B_T . These results are shown in figure 7 for the two electrode geometries. It is evident that the radiation frequency and the density calculated from it are essentially constant over the range over which the toroidal dc magnetic field is varied.

Positive Polarity

A search for microwave emission near ω_{pe} was also made for positive polarity operation of the plasma. A peak that shifted in frequency as the plasma parameters changed and which had a square root dependence on the average density was observed, but its identification with a known plasma resonance could not be positively made. The experimental results are shown in figures 8(a), 8(b), and 9, and the plasma parameters were varied as follows: Background deuterium gas pressure, 7.4×10^{-5} torr, dc toroidal magnetic field B_T , 2.4 T, and dc electrode current from 0.09 to 10.1 A.

Figure 8(a) shows the emission frequency f versus the average plasma density $\langle n_e \rangle$ measured with the microwave interferometer. The data lies along the line $f = K \langle n_e \rangle^{1/2}$, and the square root dependence of f on $\langle n_e \rangle$ is evident. The emission frequency varies from 65 to 350 MHz. For the average densities measured, this frequency range is too high to be identified with the mean ion plasma frequency, ω_{pi} and too low to correspond to the mean electron plasma frequency ω_{pe} . Figure 8(b) shows plots of n_e versus $\langle n_e \rangle$ based on assumptions that (1) $f = f_{pe}$ or (2) $f = (f_{pe} f_{pi})^{1/2}$. By assuming $f = f_{pe}$, we find that the emitting region is located at a density for which $n_e = \langle n_e \rangle / 160$, while the assumption $f = (f_{pe} f_{pi})^{1/2}$ gives $n_e = \langle n_e \rangle / 2.5$.

The dependence of the unidentified radiation frequency on the dc toroidal magnetic field B_T is shown in figure 9. The average plasma density $\langle n_e \rangle$ is held constant at $5.8 \times 10^{10} \text{ cm}^{-3}$. The radiation frequency f is essentially constant over the range of B_T .

DISCUSSION AND CONCLUSION

Measurements of the floating potential V_F and relative measurements of the radial density profile were made as functions of the radial distance into the plasma by inserting a Langmuir probe in one of the midplane regions of the plasma. Figures 10(a) and (b) show the floating potential V_F , and ion saturation voltage V_{sat} , respectively, as a function of the radial position r of the probe in the plasma, for negative polarity operation with the electrode rod inserted across the minor diameter, in a sector of the plasma other than that containing the Langmuir probe. The electrode was biased to $-2\frac{1}{2}$ kV with respect to the coil dewars. The plasma diameter is approximately 18 cm in the midplane, and the plasma axis is located approximately at a position $r = -9$ cm. Measurements of the floating potential as shown in figure 10(a) are assumed to be symmetrical about this axis. The Langmuir probe measurements were made up to a depth of $r = -4$ cm into the plasma.

The ion saturation voltage V_{sat} versus r in figure 10(b) is proportional to the plasma number density. Since the measured profile ends at $r = -4$ cm

(because of possible damage to the probe), it is extrapolated to $r = -9$ cm assuming that either (1) the profile is flat from $r = -4$ cm to $r = -9$ cm or (2) that the profile continues to extend linearly from $r = -4$ cm to $r = -9$ cm.

The radial location corresponding to the relative average density obtained from these two profiles lies at A_1 , where $r = -1.2$ cm, or at A_2 , where $r = -2.9$ cm, as shown in figure 10(b).

The electron number density n_e in the emitting region as calculated by assuming $f = f_{pe}$, was shown in figure 6(b) to be lower than the measured average density by a factor of 2.75 for negative polarity operation of the plasma. On the relative density profile curve of figure 10(b), the location of this emitting region would be represented by B_1 or B_2 , respectively, for the two different profiles assumed. B_1 and B_2 approximately correspond to $r = 2.5$ cm, a position on the periphery of the plasma where the density gradient is steep. Based on this estimate of the emitting region location, it appears that the radiation under study is essentially a surface phenomenon. In spite of this, the density calculated from the emission frequency bears a linear relationship to the average plasma density, over a wide operating range of the plasma.

It is believed that the observed radiation near ω_{pe} is caused by the generation of electron plasma waves in the plasma. These waves are assumed to be linearly converted to electromagnetic waves due to the density gradient which is especially steep near the outer periphery of the plasma (Ichimaru and Starr, 1970). The mechanism for the generation of electron plasma waves in the bumpy torus plasma is not clearly understood, especially since this plasma is known to have bulk ion temperatures T_i of about 300 to 500 eV, with electron temperatures less than $T_e = 10$ eV (Roth and Gerdin, 1970; Roth, Richardson, and Gerdin, 1976).

REFERENCES

- Adati, K., Iguchi, H., Ito, Y., and Kawabe, T. (1977) Plasma Phys. 19, 166.
- Ichimaru, S. and Starr, S. H. (1970) Phys. Rev. A 2, 821.
- Mallavarpu, R. (1977) NASA TM X-73858.
- Mallavarpu, R. and Roth, J. R. (1977) NASA TM X-73689.
- Oomens, A. A. M., Ornstein, L. Th. M., Parker, R. R., Schuller, F. C., and Taylor, R. J. (1976) Phys. Rev. Lett. 36, 255.
- Roth, J. R. (1978) IEEE Trans. Plasma Sci. PS-6, 158.
- Roth, J. R. and Gerdin, G. A. (1977) Plasma Phys. 19, 423.
- Roth, J. R. and Gerdin, G. A. (1976) NASA TN D-8211.
- Roth, J. R., Gerdin, G. A., and Richardson, R. W. (1976) IEEE Trans. Plasma Sci. PS-4, 166.
- Schrijver, H. (1973) Physica 70, 339.
- Strilchuk, A. R. and Skarsgard (1973) Can. J. Phys. 51, 195.
- Wharton, C. B. (1960) Fourth Int. Conf. on Ionization Phenomena in Gases, Uppsala Vol. II, Part III C, p. 737. North-Holland, Amsterdam.

FIGURE CAPTIONS

Figure 1. - Isometric cutaway drawing of NASA Lewis Bumpy Torus Superconducting magnet facility.

Figure 2. - Schematic of microwave emission detecting apparatus. End of rf miniature coaxial probe is located 5 to 9 cm from plasma boundary. The reentrant tube rf probe assembly is approximately 1.5 m long.

Figure 3. - Response of rf coaxial probe versus distance from plasma boundary.

Figure 4. - Location of probe with respect to the anode ring coil dewars and toroidal axis of the plasma in port 2. Magnetic field strength at probe tip is 20% of B_{\max} .

Figure 5. - Typical picture of the broad amplitude emission peak near ω_{pe} as observed on the spectrum analyzer. Electrode voltage $V_A = -2.5$ kV, $B_T = 2.4$ T, background neutral gas pressure $= 8 \times 10^{-5}$ torr, emission peak frequency $= 4.62$ GHz, horizontal scale $= 200$ MHz/div.

(a) Frequency of the emission peak f as a function of the average electron number density $\langle n_e \rangle$.

(b) Electron number density n_e from the radiation frequency f versus $\langle n_e \rangle$ for negative electrode polarities with one electrode in place and two different electrode configurations. Maximum dc magnetic field $B_T = 2.4$ T, background neutral gas pressure $= 7.4 \times 10^{-5}$ torr.

Figure 6. - Radiation characteristics for negative electrode polarity.

Figure 7. - $\langle n_e \rangle$ versus B_T for negative polarities with one electrode in place and two different electrode configurations: "D" shaped electrode and 1/4 in. stainless steel electrode rod. Average electron density was held constant. Background neutral gas pressure $= 7.4 \times 10^{-5}$ torr.

(a) Frequency of the emission peak f as a function of the average electron number $\langle n_e \rangle$.

(b) Electron number density n_e calculated by assuming (1) $f = f_{pe}$ and (2) $f = (f_{pe} f_{pl})^{1/2}$ versus $\langle n_e \rangle$ for positive electrode polarities with one "D" shaped electrode in place. Maximum dc magnetic field $B_T = 2.4$ T, background neutral gas pressure = 7.4×10^{-5} torr.

Figure 8. - Radiation characteristics for positive electrode polarity.

Figure 9. - Emission peak frequency f versus B_T for positive polarities with one "D" shaped electrode in place. Average electron density was held constant at $\langle n_e \rangle = 5.8 \times 10^{10} \text{ cm}^{-3}$, background neutral gas pressure = 7.4×10^{-5} torr.

(a) Floating potential V_F .

(b) Ion saturation voltage V_{sat} (relative number density) versus the radial distance r into the plasma as measured by a Langmuir probe for negative polarities with one 1/4 in. electrode rod in place. Electrode voltage $V_A = -2\frac{1}{2}$ kV, maximum dc magnetic field $B_T = 2.4$ T, background neutral gas pressure = 7.4×10^{-5} torr.

Figure 10. - Radial profiles of plasma characteristics.

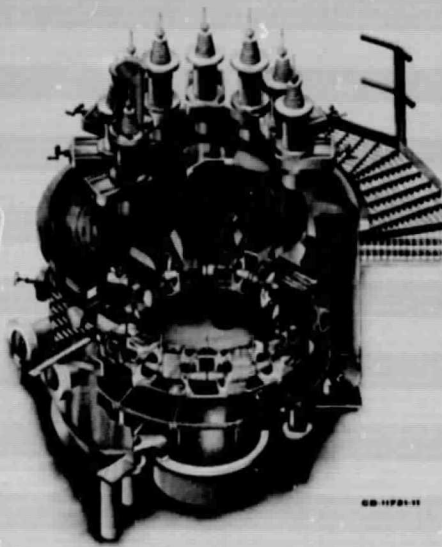


Figure 1. - Isometric cutaway drawing of NASA Lewis bumpy torus superconducting magnet facility.

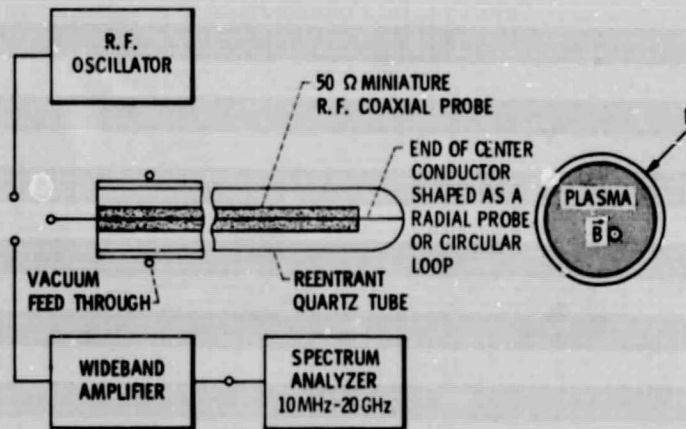


Figure 2. - Schematic of R. F. emission detecting apparatus. Tip of R. F. miniature coaxial probe is located 5-9 cms from plasma boundary. The re-entrant tube-R. F. probe assembly is approximately 1.5 m long.

ORIGINAL PAGE IS
OF POOR QUALITY

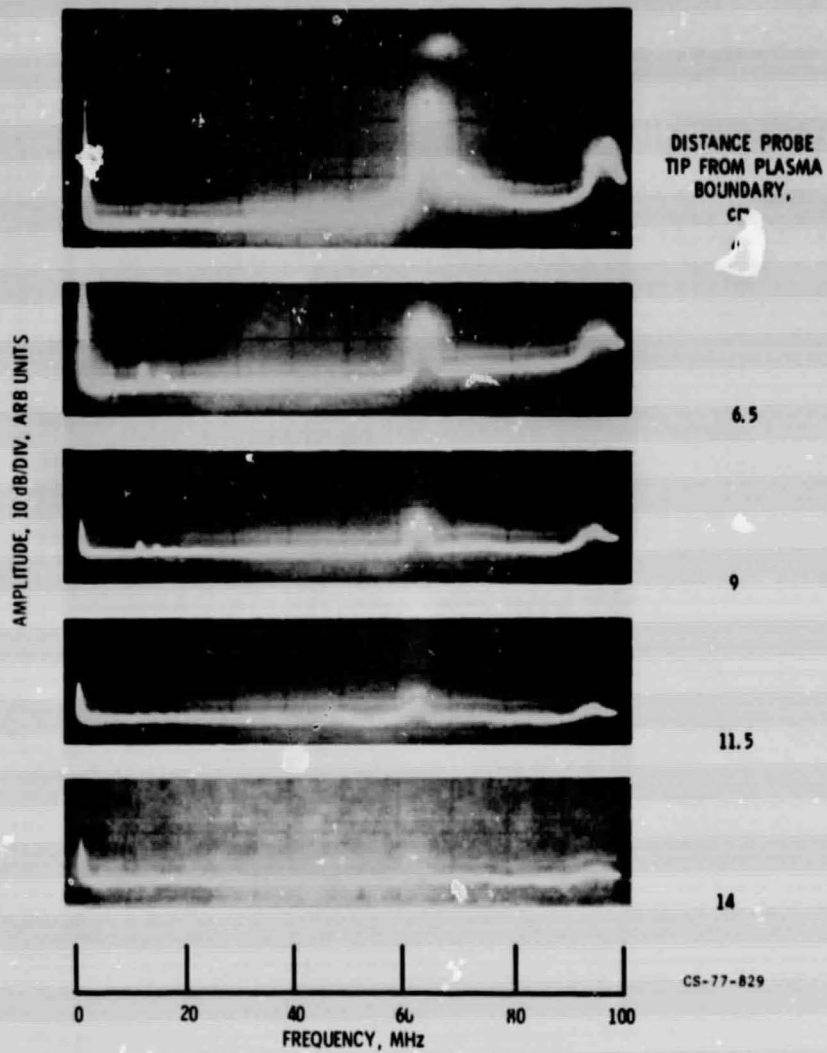


Figure 3. - Response of R F coaxial probe versus distance from plasma boundary.

ORIGINAL PAGE IS
OF POOR QUALITY

CONTOUR	NORMALIZED MAGNETIC FIELD STRENGTH	CONTOUR	NORMALIZED MAGNETIC FIELD STRENGTH
A	0.050	Q	0.850
B	.100	R	.900
C	.150	S	.950
D	.200	T	1.000
E	.250	U	1.050
F	.300	V	1.100
G	.350	W	1.150
H	.400	X	1.200
I	.450	Y	1.250
J	.500	Z	1.300
K	.550	1	1.350
L	.600	2	1.400
M	.650	3	1.450
N	.700	4	1.500
O	.750	5	1.550
P	.800	6	1.600

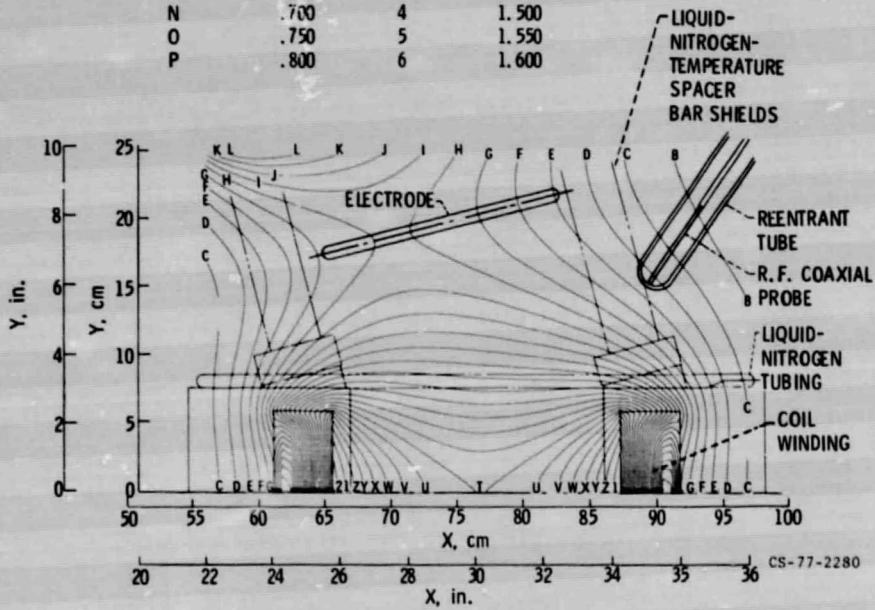


Figure 4. - Location of probe with respect to the anode ring, coil dewars, and toroidal axis of the plasma in port 2. Magnetic field strength at probe tip is 20% of B_{max} .

ORIGINAL PAGE IS
OF POOR QUALITY

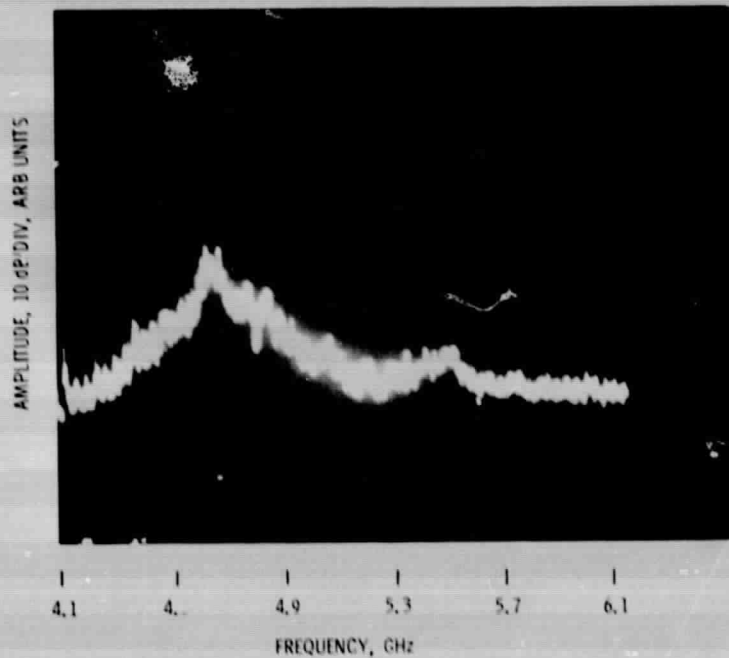
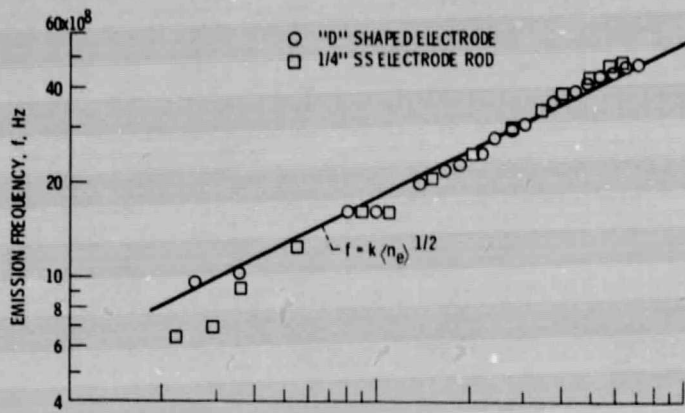
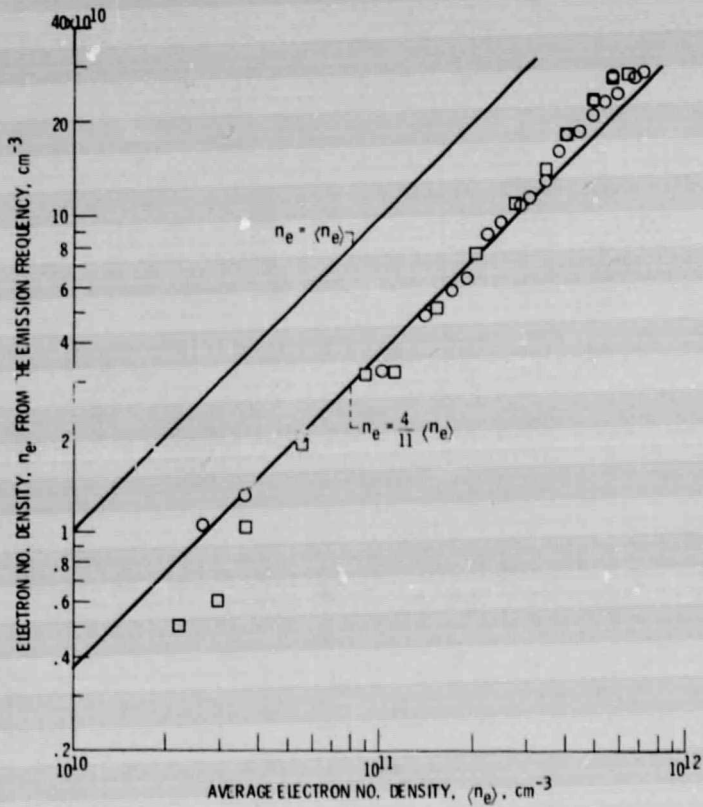


Figure 5. - Typical picture of broad amplitude emission peak near ω_{pe} as observed on spectrum analyzer. Electrode voltage $V_A = -2.5$ KV, $B_T = 2.4$ tesla, background neutral gas pressure = 8×10^{-5} torr. Emission peak frequency, 4.62 GHz. Horizontal scale, 200 MHz/div.



(a) FREQUENCY OF THE EMISSION PEAK f AS A FUNCTION OF THE AVERAGE ELECTRON NUMBER DENSITY $\langle n_e \rangle$.



(b) ELECTRON NUMBER DENSITY n_e FROM THE RADIATION FREQUENCY f , VERSUS $\langle n_e \rangle$ FOR NEGATIVE ELECTRODE POLARITIES WITH ONE ELECTRODE IN PLACE AND TWO DIFFERENT ELECTRODE CONFIGURATIONS. MAXIMUM D.C. MAGNETIC FIELD $B_T = 2.4$ tesla. BACKGROUND NEUTRAL GAS PRESSURE $= 7.4 \times 10^{-5}$ torr.

Figure 6. - Radiation characteristics for negative electrode polarity.

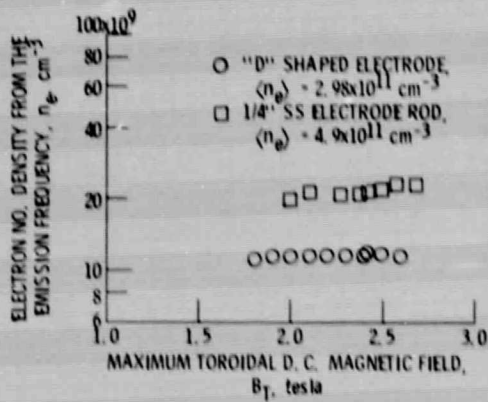
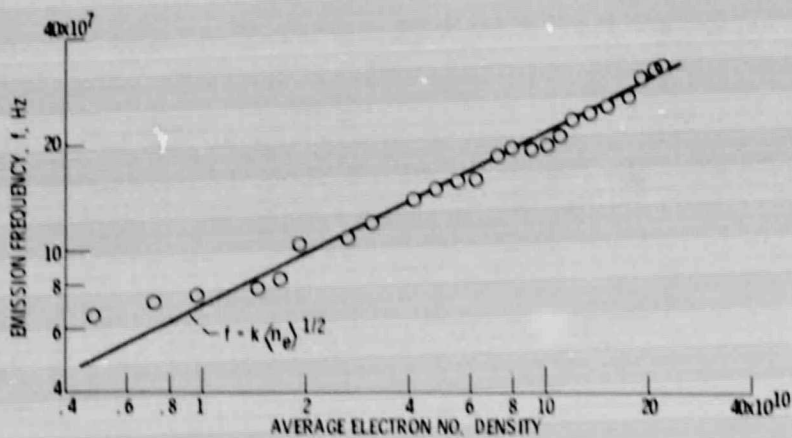


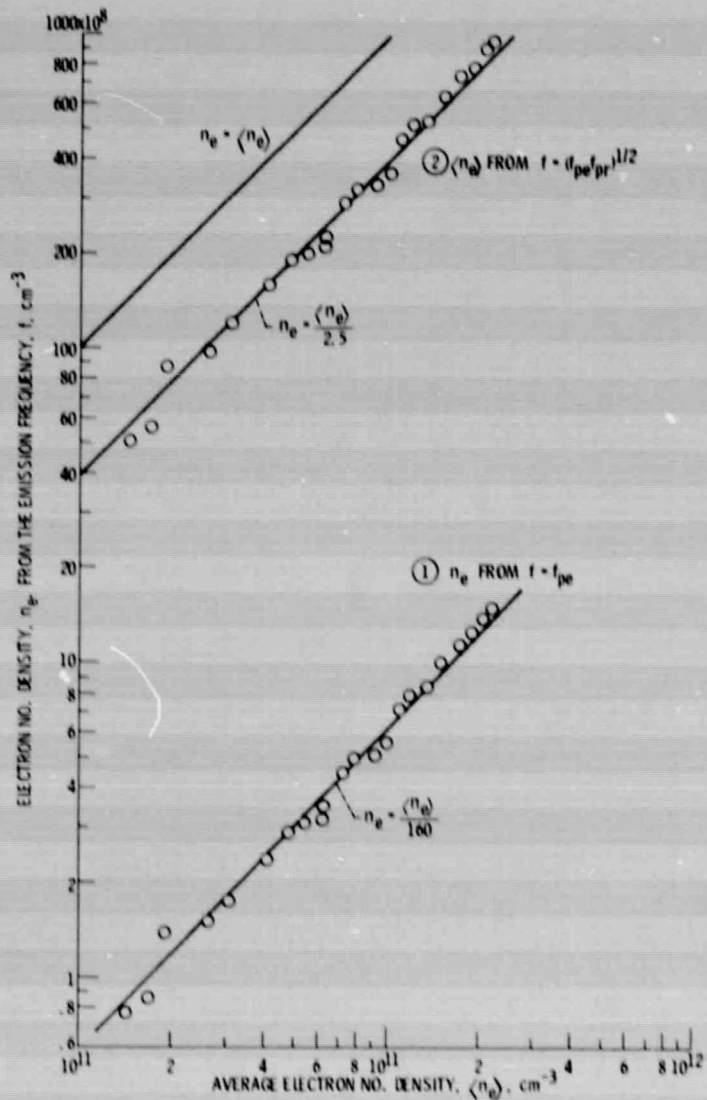
Figure 7. - $\langle n_e \rangle$ versus B_T for negative polarities with one electrode in place and two different electrode configurations: "D" shaped electrode and 1/4" stainless steel electrode rod. Average electron density was held constant. Background neutral gas pressure = 7.4×10^{-5} torr.



(a) FREQUENCY OF THE EMISSION PEAK f AS A FUNCTION OF THE AVERAGE ELECTRON NUMBER DENSITY $\langle n_e \rangle$.

Figure 8. - Radiation characteristics for positive electrode polarity.

IT-7606



(1) ELECTRON NUMBER DENSITY n_e CALCULATED BY ASSUMING (1) $f = f_{pe}$ AND (2) $f = (f_{pe} f_{pr})^{1/2}$, VERSUS $\langle n_e \rangle$ FOR POSITIVE ELECTRODE POLARITIES WITH ONE "D" SHAPED ELECTRODE IN PLACE. MAXIMUM D. C. MAGNETIC FIELD $B_T = 2.4$ tesla. BACKGROUND NEUTRAL GAS PRESSURE $= 7.4 \times 10^{-5}$ torr.

Figure 8. - Concluded.

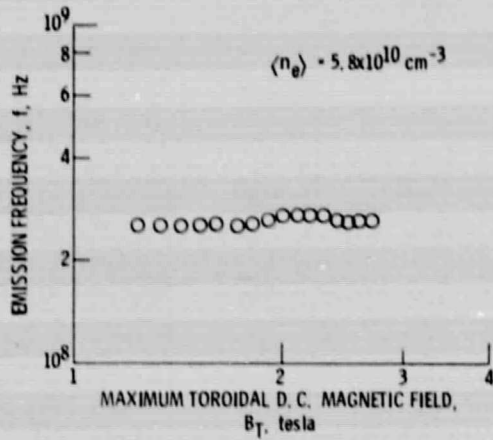
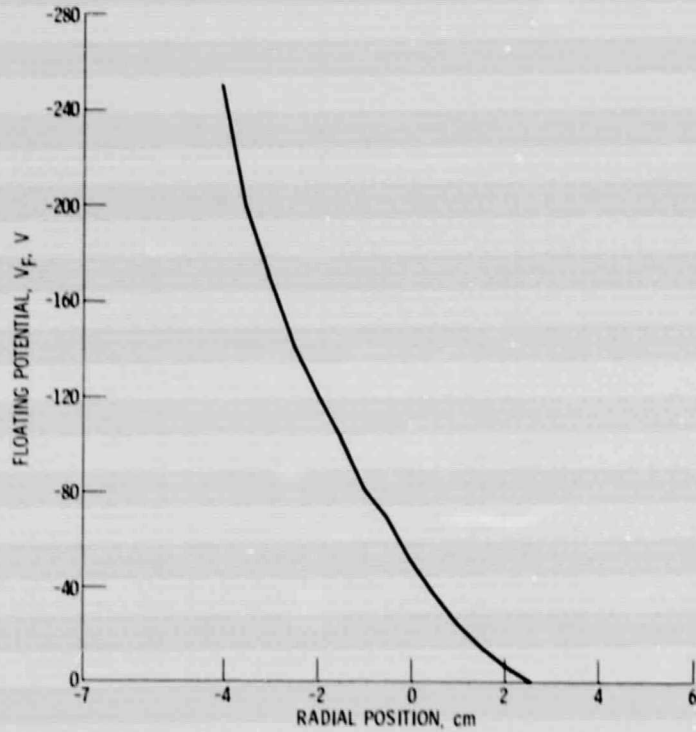
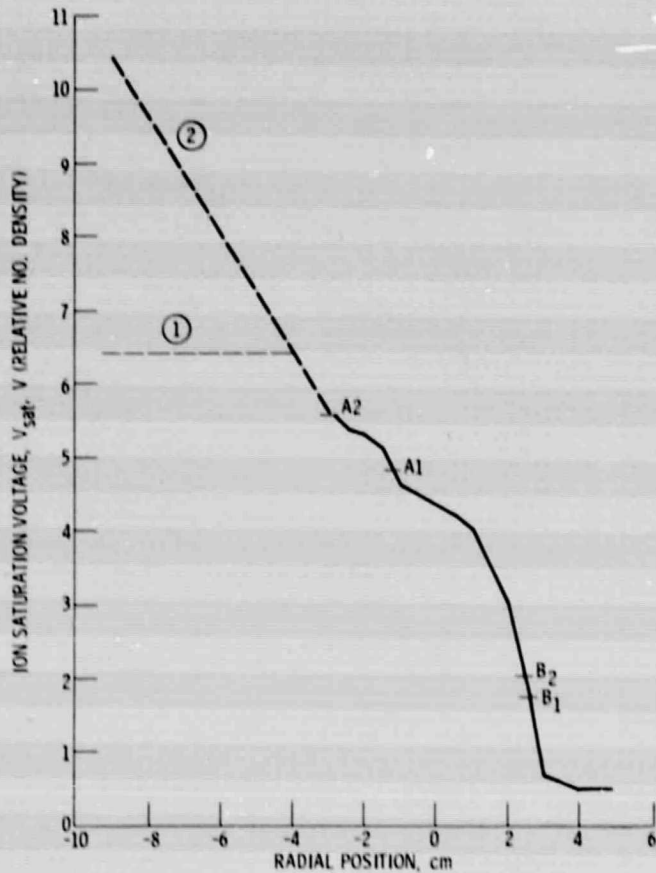


Figure 9. - Emission peak frequency f versus B_T for positive polarities with one "D" shaped electrode in place. Average electron density was held constant at $\langle n_e \rangle = 5.8 \times 10^{10} \text{ cm}^{-3}$. Background neutral gas pressure = 7.4×10^{-5} torr.



(a) FLOATING POTENTIAL V_F .

Figure 10. - Radial profiles of plasma characteristics.



(b) ION SATURATION VOLTAGE V_{sat} (RELATIVE NUMBER DENSITY) VERSUS THE RADIAL DISTANCE r INTO THE PLASMA AS MEASURED BY A LANGMUIR PROBE FOR NEGATIVE POLARITIES WITH ONE 1/4" ELECTRODE ROD IN PLACE. ELECTRODE VOLTAGE $V_A = -24$ kV, MAXIMUM D. C. MAGNETIC FIELD $B_T = 2.4$ tesla AND BACKGROUND NEUTRAL GAS PRESSURE $= 7.4 \times 10^{-5}$ torr.

Figure 10. - Concluded.

1. Report No. NASA TM-78940	2. Government Accession No.	3. Recipient's Catalog No.	
4. Title and Subtitle MICROWAVE RADIATION MEASUREMENTS NEAR THE ELECTRON PLASMA FREQUENCY OF THE NASA LEWIS BUMPY TORUS PLASMA		5. Report Date	
		6. Performing Organization Code	
7. Author(s) R. Mallavarpu and J. R. Roth		8. Performing Organization Report No. E-9686	
		10. Work Unit No.	
9. Performing Organization Name and Address National Aeronautics and Space Administration Lewis Research Center Cleveland, Ohio 44135		11. Contract or Grant No.	
		13. Type of Report and Period Covered Technical Memorandum	
12. Sponsoring Agency Name and Address National Aeronautics and Space Administration Washington, D.C. 20546		14. Sponsoring Agency Code	
		15. Supplementary Notes	
16. Abstract <p>Microwave emission near the electron plasma frequency of the NASA Lewis Bumpy Torus plasma has been observed, and its relation to the average electron density and the dc toroidal magnetic field was examined. The emission was detected using a spectrum analyzer and a 50 Ω miniature coaxial probe. The radiation appeared as a broad amplitude peak that shifted in frequency as the plasma parameters were varied. The observed radiation scanned an average plasma density ranging from $2 \times 10^{10} \text{ cm}^{-3}$ to $8 \times 10^{11} \text{ cm}^{-3}$. A linear relation was observed between the density calculated from the emission frequency and the average plasma density measured with a microwave interferometer. With the aid of a relative density profile measurement of the plasma, it was determined that the emissions occurred from the outer periphery of the plasma.</p>			
17. Key Words (Suggested by Author(s)) Plasma emission Electron plasma frequency		18. Distribution Statement Unclassified - unlimited STAR Category 75	
19. Security Classif. (of this report) Unclassified	20. Security Classif. (of this page) Unclassified	21. No. of Pages	22. Price*